

A novel methodology for large scale, daily assessment of the direct radiative forcing of smoke aerosols

E. T. Sena¹ and P. Artaxo¹

[1]{Institute of Physics, University of São Paulo, São Paulo, Brazil}

Correspondence to: E. T. Sena (elisats@if.usp.br)

Abstract

A new methodology was developed for obtaining daily retrievals of the direct radiative forcing of aerosols (24h-DARF) at the top of the atmosphere (TOA) using satellite remote sensing. Simultaneous CERES (Clouds and Earth's Radiant Energy System) shortwave flux at the top of the atmosphere (TOA) and MODIS (Moderate Resolution Spectroradiometer) aerosol optical depth (AOD) retrievals were used. To analyse the impact of forest smoke on the radiation balance, this methodology was applied over the Amazonia during the peak of the biomass burning season from 2000 to 2009.

To assess the spatial distribution of the DARF, background smoke-free scenes were selected. The fluxes at the TOA under clean conditions (F_{cl}) were estimated as a function of the illumination geometry (θ_0) for each $0.5^\circ \times 0.5^\circ$ degree grid cell. The instantaneous DARF was obtained as the difference between the clean ($F_{cl}(\theta_0)$) and the polluted flux at the TOA measured by CERES in each cell ($F_{pol}(\theta_0)$). The radiative transfer code SBDART (Santa Barbara DISORT Radiative Transfer model) was used to expand instantaneous DARFs to 24h averages.

This new methodology was applied to assess the DARF both at high temporal resolution and over a large area in Amazonia. The spatial distribution shows that the mean 24h-DARF can be as high as -30 W/m^2 over some regions. The temporal variability of the 24h-DARF along the biomass burning season was also studied and showed large intraseasonal and interannual variability. We showed that our methodology considerably reduces statistical sources of uncertainties in the estimate of the DARF, when compared to previous approaches. DARF

assessments using the new methodology agree well with ground-based measurements and radiative transfer models. This demonstrates the robustness of the new proposed methodology for assessing the radiative forcing for biomass burning aerosols. To our knowledge, this was the first time satellite remote sensing assessments of the DARF were compared with ground based DARF estimates.

1 Introduction

The Amazonia is the largest tropical rainforest of the world, occupying an area of more than 6.6 million km² in South America. This large ecosystem plays a crucial role in regulating global and regional climate and the hydrological cycle, powering global atmospheric circulation, transporting heat and moisture to continental areas (Davidson and Artaxo, 2004, Artaxo et al., 2013). In the last decades, anthropogenic activities, such as deforestation for agricultural and urban expansion have highly disturbed this environment (Betts et al., 2008, Bowman et al., 2009, Davidson et al., 2012). During the wet season, the Amazon Basin is one of the few continental places of the world where we can observe pristine conditions (Andreae et al., 2007). The population of aerosols during the wet season is dominated by primary biogenic coarse mode particles (Martin et al., 2010), and presents typical concentration of about 300 particles per cm³ (Artaxo et al., 2002). This scenario changes dramatically during the dry season, with particle concentration reaching around 20,000 particles per cm³ due to biomass burning emissions (Holben et al., 1996, Echalar et al., 1998, Andreae et al., 2002, Artaxo et al., 2009). This strong increase in aerosol concentration is accompanied by a significant modification in particle size distribution, since most of the particles emitted during burning events belong to the fine mode (Dubovik et al., 2002, Eck et al., 2003, Schafer et al., 2008).

Aerosol particles can modify the Earth's radiative balance in two ways: i) directly, by interacting with solar radiation, through scattering and absorption processes (eg., Charlson et al., 1992, Chylek and Wong, 1995), and ii) indirectly, by modifying the microphysical structure of clouds, such as droplet size distribution and cloud albedo (eg., Twomey et al., 1977, Coakley et al., 1987, Albrecht et al., 1989, Andreae et al., 2004, Koren et al., 2008). These effects depend on the concentration and on the horizontal and vertical distributions of particles in the atmosphere, on their optical properties, such as single scattering albedo, size

1 distribution, phase function, hygroscopicity, and on the surface reflectance properties of the
2 underlying region (eg., Haywood and Boucher, 2000; Yu et al., 2006). In particular, biomass
3 burning aerosols play an important role in modifying the radiative energy balance of the
4 affected region because fine mode particles interact efficiently with solar radiation (Liou,
5 2002).

6 The direct aerosol radiative forcing (DARF) in Amazonia was previously assessed using
7 radiative transfer models coupled with ground-based remote sensing measurements (Procopio
8 et al., 2004) or in-site field-campaigns (Ross et al., 1998). Although these approaches may
9 provide detailed insight about a specific burning event, they are limited in space (in the case
10 of ground-based studies) or in time (in the case of intensive field campaigns). As satellite
11 remote sensing provides high spatial coverage it has been used to assess the large scale
12 DARF. An interesting technique used CERES (Clouds and Earth's Radiant Energy System)
13 flux at the top of the atmosphere (TOA) combined with MODIS (Moderate Resolution
14 Spectroradiometer) or MISR (Multi-angle Imaging Spectroradiometer) aerosol optical depth
15 (AOD) to assess the mean DARF over Amazonia during the biomass burning season and
16 analyze its spatial variability (Patadia et al., 2008, Sena et al., 2013). This technique
17 (CERES+MODIS) has also been widely applied to evaluate the mean DARF over a time
18 period (usually 2-3 months) in several other regions (eg., Zhang et al., 2005, Christopher,
19 2011, Feng and Christopher, 2014, Sundström et al., 2014). Although these studies focused on
20 averages are useful, they lack the high temporal resolution needed to observe important
21 details on the changes of the radiative balance due to the short residence time of aerosols in
22 the atmosphere. During the dry season, aerosol residence time within the boundary layer is
23 estimated to be about 4 to 6 days (Freitas et al., 2005, Edwards et al., 2006). Also, biomass
24 burning aerosols can be transported over great distances away from their sources (Andreae et
25 al., 2001, Longo et al., 2009), depending on the prevalent dynamics in the studied area. Due
26 to their short lifetime and to the dynamics of transport of these particles, aerosols present
27 highly inhomogeneous spatial and temporal distributions. With that in mind, we developed a
28 methodology for calculating the smoke DARF in Amazonia with higher spatial and temporal
29 resolution than previous assessments ($0.5^\circ \times 0.5^\circ$ degrees and 1 day, respectively) using
30 satellite remote sensing. As opposed to previous studies, that consider the total effect of
31 aerosols (both from background and polluted conditions) on the radiative budget, this study
32 focused on assessing the anthropogenic DARF only. This can also be regarded as an

improvement over previous methodologies, since aerosol-free conditions cannot be observed in the atmosphere.

The main goals of this work were:

i) to introduce a new methodology to assess the daily direct radiative forcing of biomass burning aerosols over a large scale of Amazonia using satellite remote sensing (Section 2);

ii) to analyse the intraseasonal and interannual variability of the daily average DARF as well as its mean daily spatial distribution pattern over Amazonia (Sections 3.1 and 3.2);

iii) to validate the calculated DARF obtained by applying this new methodology with ground-based sensors, as well as radiative transfer DARF calculations (Section 4).

We also believe that this methodology could be easily applied to study the DARF_{24h} in other regions of the world, impacted by biomass burning or even urban pollution.

2 Data and methods

In this work, combined CERES shortwave TOA flux and MODIS aerosol optical depth (AOD) at 550 nm were used to assess the direct radiative forcing of biomass burning aerosols over the Amazon Basin for cloud-free conditions. These both instruments are aboard NASA's Terra and Aqua satellites.

CERES sensors are passive scanning radiometers that measure the upward radiance in three broadband channels: i) between 0.3 to 5.0 μm , to measure the shortwave radiation reflected in the solar spectrum; ii) between 8 and 12 μm , to measure the thermal radiation emitted by the Earth in the atmospheric window spectral region, and iii) between 0.3 and 200 μm to measure the total radiation spectrum emerging at the TOA (Wielicki et al., 1996). Radiance measurements are converted into broadband radiative fluxes through the use of angular distribution models (ADMs) (Loeb et al., 2005).

MODIS measures the radiance at the TOA in 36 narrow spectral bands between 0.4 and 14.4 μm (Salomonson et al., 1989). Among its various applications, MODIS observations have been widely used to monitor land surface, oceans and atmosphere properties and to provide

information about cloud and aerosol optical properties, their spatial and temporal variations, and the interaction between aerosols and clouds (King et al., 1992).

CERES Single Scanner Footprint (CERES-SSF) product provides simultaneous retrievals of the upward flux at the TOA derived by CERES on three broadband channels, and properties of aerosols and clouds reported by MODIS. In this product, MOD04 aerosol and cloud properties, that are originally reported with a 10 km spatial resolution, are reprojected to CERES 20 km resolution (Smith, 1994). Over land, MODIS's AOD uncertainty is estimated as: $\sigma_{land} = \pm 0.05 \pm 0.15 AOD_{550nm}$ (Remer et al., 2005).

For the development of the new methodology presented here, we used CERES-SSF Edition 3A shortwave flux retrievals at the TOA from Terra satellite over the Amazon Basin from July 1 to October 31 from 2000 to 2009. The studied area was limited between the coordinates 3°N–20°S, 45°W–65°W and 3°N–11°S, 65°W–74°W. Pixels with 1-km resolution MODIS cloud fraction above 0.5% and with a clear area in the MODIS 250 m resolution lower than 99.9% were removed. To limit distortions we removed from our analysis pixels that presented view and solar zenith angles greater than 60°. The DARF was calculated with a 0.5° x 0.5° latitude/longitude spatial resolution, according to the methodology described in the next section.

2.1 Evaluation of the daily direct RF of biomass burning aerosols

The direct radiative forcing of aerosols (DARF) can be defined as the difference between the upward radiation flux at the TOA measured in background (F_{cl}) and polluted conditions (F_{pol}).

$$DARF = F_{cl} - F_{pol} . \quad (1)$$

For each scene observed by CERES, F_{pol} can be directly obtained from the mean flux at the TOA for each 0.5° x 0.5° grid cell. To calculate the instantaneous DARF, we need to estimate what would be the flux at the TOA for background conditions (F_{cl}) for the same illumination geometry of the polluted scene. To perform this estimate, scenes that presented aerosol optical depth (AOD) smaller than 0.1 were selected, and considered as background scenes. This threshold was selected by analysing AERONET's AOD during the wet season. For each cell, the flux at the TOA observed for background scenes (F_{cl}) during the 40-months studied period was plotted against the cosine of the solar zenith angle ($\cos(\theta_0)$). An example of this plot, for

the grid cell centred at latitude 8.75°S and longitude 53.75°W, is shown in Figure 1. A correlation coefficient of 0.94 between F_{cl} and $\cos(\theta_0)$ was observed for the data points within this cell indicating the adequacy of the linear approximation. It is worth emphasizing that this example is not a best case scenario. In fact, more than 80% of the cases analysed showed a correlation larger than 0.90 between F_{cl} and $\cos(\theta_0)$.

The solar zenith angle varied from about 10° to 52° at Terra satellite passage time over the Amazonia during the study period. For this solar zenith angle range, F_{cl} varies linearly with $\cos(\theta_0)$. By adjusting a linear fit to the data points within each cell we can calculate $F_{cl}(\theta_0)$ for any illumination geometry, according to equation 2,

$$F_{cl}(\theta_0) = A \cos(\theta_0) + B, \quad (2)$$

where A and B correspond to the slope and the intercept of the linear fit, respectively.

To assess the instantaneous DARF, the mean solar zenith angle within each cell during the satellite passage time was identified for every polluted scene. For each cell, the instantaneous DARF was evaluated as the difference between $F_{cl}(\theta_0)$ and the mean flux at the TOA retrieved by CERES in polluted conditions ($F_{pol}(\theta_0)$), as previously stated in equation (1). The uncertainty of the DARF in each cell (σ_{DARF}), was computed using error propagation, according to the following equation:

$$\sigma_{DARF}^2 = \sigma_A^2 \cos^2(\theta_0) + \sigma_B^2 + 2 \text{cov}(A, B) \cos(\theta_0) + \sigma_{Fpol}^2, \quad (3)$$

where σ_A , σ_B and $\text{cov}(A, B)$ are the uncertainty of the slope, intercept and the covariance between the slope and the intercept, respectively; σ_{Fpol} is the uncertainty of the flux in each cell for the polluted condition.

2.2 Correction of the DARF according to empirical ADMs

As already discussed, to convert CERES radiance measurements to radiative flux at the TOA it is necessary to define the angular distribution models (ADMs) for different scenes (Loeb et al., 2005). In a recent work, Patadia et al. (2011) pointed out that the angular distribution models currently used by CERES team to derive shortwave fluxes at the TOA over land in cloud-free conditions do not take into account aerosol properties in the observed scene. This

can result in large errors in the shortwave fluxes derived by this sensor for areas with high concentrations of aerosols, such as the Amazonia during the biomass burning season. To estimate the impact of the anisotropy caused by high aerosol loading on the flux at the TOA, Patadia et al. (2011) developed a methodology to obtain new empirical angular distribution models for the Amazon Basin region during the dry season. The authors used radiance measurements obtained by CERES shortwave channel over the Amazonia for different view and solar illumination geometries between 2000 and 2008. In a later work they have assessed the difference between the DARF evaluated using both, CERES ADMs and their new empirical ADMs (Patadia and Christopher, 2014). They have found that, on average, CERES DARF relates to the corrected DARF calculated with their empirical ADMs, according to the following equation:

$$DARF_{corrected} = DARF - 52.27AOD - 2.71 + 35.15AOD + 1.78. \quad (4)$$

The correction proposed by Patadia and Christopher (2014) was applied to the CERES-MODIS DARF estimates introduced in the previous section.

A discrete-ordinate radiative transfer (DISORT) code (Stamnes et al., 1988) was used to expand the instantaneous radiative forcing, calculated for the satellite passage time, to 24 hours averages. MODIS BRDF/Albedo Model (MCD43B1) retrievals (Schaaf et al., 2002) over the studied area were used to develop the surface albedo models used in the radiative transfer calculations. Aerosol optical properties retrieved by the AERONET (Aerosol Robotic Network) ground-based sun-photometers (Dubovik and King, 2000) located in the Amazonia during the dry season were also used in this computation. For a detailed description of the methodology used to perform this expansion please refer to Sena et al. (2013).

3 Results and discussions

In this section we will present and explore the main results obtained by applying the methodology introduced in section 2.1 to assess the DARF. Some examples of the spatial distribution and the temporal variability of the 24h-DARF along the biomass burning season are shown and discussed in the next subsections. In section 3.3, the average of the DARF during the biomass burning season of each year is computed and compared with previous DARF results.

3.1 Examples of the spatial distribution of the 24-h DARF

In Brazil, most fires occur on the Southern and Eastern borders of the Amazon Basin, in a region known as the “arc of deforestation” (Malhi et al., 2008, Morton et al., 2008). During the dry season low level Easterly winds are dominates the atmospheric circulation over central South America (Nobre et al., 1998) . Due to this dynamical feature, smoke particles are transported towards the forest and the Andes mountain range, where eventually wind direction changes (Freitas et al., 2009). Biomass burning aerosols can be transported over long distances away from their sources (Andreae et al., 2001, Freitas et al., 2005, Longo et al., 2009, Mishra et al., 2015) and cover large areas of up to millions of km² (Prins et al., 1998). Aerosol transport during the biomass burning season can significantly modify the spatial distribution of the DARF from one day to another. Two examples of the spatial distribution of the 24-h DARF, for 08/13/2005 and 08/15/2005, are shown in Figure 2, with their respective uncertainties. Composite images from MODIS’s red, blue and green spectral channels, are also shown in this figure.

Figure 2 shows that, on August 13th, 2005, the smoke plume covers a large area of the Brazilian Amazonia, between 4°S and 12°S and 55° and 70°W. The 24-h DARF over the area was particularly high for that day, varying from about -30 to -15 W/m². On August 15th, 2005, we note that the smoke plume has moved Southeast, following the Andes mountain range line, strongly impacting the Southern Amazonia, Western Bolivia and Northern Paraguay. The area located between 8°S and 20°S and 57°W and 65°W showed the highest 24-h DARF values for that day, also ranging from -30 to -15 W/m². The 24h-DARF showed in Figure 2b was, on average, -14.3 ± 0.3 W/m² on August 13th and -15.6 ± 0.3 W/m² on August 15th. These results clearly show the importance of wind circulation in the transport of aerosol plumes and how atmospheric dynamics may influence the shortwave radiative balance of the region.

3.2 Temporal variability of the DARF along the biomass burning season

Due to the short lifetime of aerosols in the atmosphere, the DARF may vary largely along the 2-months of the biomass burning season. To analyze this temporal variability, the average of the 24-h DARF over the studied area was calculated for each day of the year. Examples of the time series of the mean daily DARF during the biomass burning season from 2000 to 2009 are

illustrated in Figure 3. Due to a problem in CERES-SSF data processing, the year 2004 presents a high amount of missing values for aerosol and cloud properties in its database. Therefore this year was not included in Figure 3, nor in the forthcoming analysis.

Figure 3 shows that, besides its large interannual variability, the DARF also varies widely along the biomass burning season. Different temporal patterns along the biomass burning season are observed depending on the year. For example, for most of 2005's dry season, the DARF showed little variation, averaging around $-9 \pm 2 \text{ W/m}^2$. On the other hand, in 2007, the DARF became gradually more negative, starting around 0 W/m^2 in the beginning of August and reaching values of the order of -25 W/m^2 at the end of September. However, 2005 and 2007, both, present similar mean 24-h DARF during the burning season, as will be shown in the next section (Figure 4). The temporal variation pattern during the biomass burning season of 2006 presents an intermediate trend to those observed in 2005 and 2007. In 2006, the DARF decreases until the beginning of September, when it saturates and finally increases once again.

The interannual variability of the DARF can also be observed. The impact of smoke aerosols in the radiative balance of 2005 and 2007 was very pronounced, while the DARF was very close to zero during the whole biomass burning season of 2009. Changes in rainfall patterns play a major role to the interannual variability of the DARF. The high DARFs in 2005 and 2007 are associated with severe droughts that contributed to forest and savanna fires and high aerosol loadings in these years (Marengo et al., 2008, Ten Hove et al., 2012). On the other hand, the rainfall over the Amazonia in 2009 was extremely high (Satyamurty et al., 2013), which contributed to the decrease in the number of fire sources and the efficient removal of smoke aerosols from the atmosphere.

The daily DARF variations from one day to another, shown in this figure, are mainly due to changes at the MODIS imaged area, that varies according to the satellite track. Due to its polar orbiting track, every day the scanned area slightly changes, finally repeating itself after about 16 days. Depending on Terra track, for some cases MODIS doesn't cover areas heavily impacted by smoke aerosols, and the mean 24h-DARF could be underestimated. The daily DARF variation is also influenced by changes in fire sources location, transport and cloud coverage along the biomass burning season.

3.3 Average of the DARF during the biomass burning season

In previous studies (Patadia et al., 2008, Sena et al., 2013), the average of the direct radiative forcing of aerosols during the biomass burning season over the Amazonia was also calculated by using CERES and MODIS sensors. In those approaches, the average flux for clean conditions during the biomass burning season ($BBSF_{cl}$) for each cell grid was estimated from the intercept of the regression between TOA fluxes and AOD retrievals from August to September. The mean DARF during the biomass burning season ($BBSDARF$) was then calculated by subtracting the mean flux at the TOA ($BBSF_{pol}$) from the mean flux for clean conditions ($BBSF_{cl}$) observed as averages during this two-month study period. The DARF calculated using this methodology considers the total effect of aerosols. Since the flux for clean conditions (F_{cl}) is defined for $AOD=0$, the effect of smoke aerosols cannot be isolated from the effect of background aerosols. Thus the total effect of aerosols from both background and polluted conditions are included in the $BBSDARF$.

The new methodology introduced here (Section 2.1), provides the 24h-DARF for each individual day, with a much higher temporal resolution than the one used in previous studies. Furthermore this new methodology considers a more realistic clean condition, by defining F_{cl} in the presence of background aerosols. Since background aerosols are always present in the atmosphere, the contribution of background aerosols to the radiative balance should not be considered as forcing in the strict sense. In fact, some authors define the contribution of background + polluted aerosols as the direct radiative effect instead of direct radiative forcing (eg., Yu et al., 2006).

In this section we compared the DARF obtained using the new methodology introduced in section 2.2 with the seasonal DARF values calculated previously by Sena et al., 2013. For this comparison, the daily DARF, obtained in this work, was averaged between the months of August and September of each year ($\langle 24hDARF \rangle_{BBS}$). To ensure that we make a fair comparison, the corrections proposed by Patadia and Christopher (2014), and used for the evaluation of the 24h-DARF in this paper (Section 2.2), were also applied a posteriori to the Sena et al., 2013 seasonal forcing ($BBSDARF$). Figure 4 shows the mean AOD at 550 nm during the biomass burning, and the comparison between $\langle 24hDARF \rangle_{BBS}$ and $BBSDARF$, calculated over the studied area, from 2000 to 2009. Once again, 2004 was excluded from the analysis, due to CERES-SSF database problems discussed in the previous section.

Figure 4 shows that the $\langle 24hDARF \rangle_{BBS}$ is always lower than the BBSDARF. The average of the BBSDARF for this 10-year period (2000 to 2009) is $-8.2 \pm 2.1 \text{ W/m}^2$, while the 10-year average of the $\langle 24hDARF \rangle_{BBS}$ is $-5.2 \pm 2.6 \text{ W/m}^2$. Two factors contribute to this difference: i) different references were used at the assessment of the clean flux, F_{cl} , in each methodology (AOD=0 vs. background conditions), and ii) CERES-SSF product provides an older MOD04 collection before 2005, and this strongly affects BBSDARF retrievals. In the following paragraphs, these DARF differences and their sources will be further explored.

SBDART (Santa Barbara DISORT Radiative Transfer model) (Richiazzi et al., 1998) calculations suggest that the contribution of background aerosols at AOD=0.1 to the 24h-DARF over the Amazonia is about -2 W/m^2 . Hence, the contribution of background aerosols may explain the magnitude of the differences in the radiative forcings obtained from 2005 on, but not before that year. Part of the DARF differences observed from 2000 to 2003, are very likely associated with the aerosol optical properties contained in CERES-SSF product, Edition 3A, used both in this work and by Sena et al. (2013). This product provides aerosol optical properties calculated using MODIS aerosol algorithm MOD04 - collection 4 until mid-2005, and MOD04 - collection 5 after that date. A major difference between aerosol optical depths obtained by these two collections is due to the fact that collection 4 does not allow negative values of AOD, while for collection 5, the lowest limit for the AOD is -0.05, to account for the uncertainty of the retrieved AOD. Therefore, for low aerosol loading, when AOD from MOD04 - collection 4 is projected to CERES lower resolution, it may be overestimated, since negative AOD values were removed from the average. Thus, when applying the methodology used by Patadia et al. (2008) and Sena et al. (2013), to CERES-SSF data that contained MOD04 - collection 4 AOD, the $BBSF_{cl}$ is underestimated and, therefore, the BBSDARF is overestimated (Figure 5). This explains the differences between both DARF evaluations observed in Figure 4.

The solar zenith angle strongly influences the upward flux at the TOA (F_{TOA}). CERES fluxes retrievals obtained over the same surface, for the same aerosol loading and same atmospheric conditions, and at different illumination geometry will present different F_{TOA} . In the previous methodology used in Sena et al., 2013, two months of data were used to estimate the BBSDARF through the linear fit of F_{TOA} by AOD. Thus, flux measurements performed on different days and at different times (and therefore different solar zenith angles) contributed to

increase the dispersion of the points on the y axis, increasing the uncertainty of BBSDARF. In the new methodology, the DARF is obtained as a function of the solar zenith angle, which eliminates the noise caused by solar zenith angle variations, observed in previous studies. This was another important improvement of the methodology proposed in this work over the previously used methodology.

It is also important to emphasize that both methodologies are applied only in cloud-free conditions. MODIS Level 3 cloud fraction retrievals indicate that during the study period (August to September) the cloud fraction over Amazonia is on average about 47%, during Terra morning passage (about 10:30 AM LT), increasing to about 56%, during the afternoon (Aqua passage time is about 1:30 PM LT). Therefore, the mean $\langle 24hDARF \rangle_{BBS}$ over the whole study area weighted by cloud cover is about -2.6 W/m^2 .

The mean correlation between the AOD 550 nm and the $\langle 24hDARF \rangle_{BBS}$ from 2000 to 2009 is -0.86 ± 0.03 , which is better than the mean correlation between the AOD and BBSDARF previously obtained, of -0.75 ± 0.05 . This is another indication that the new daily methodology proposed here is more robust to evaluate the DARF than the seasonal averaged methodology used in previous studies.

4 Comparison between satellite and ground-based direct radiative forcing

The methodology proposed in this work uses upward TOA flux estimates from CERES-MODIS sensors aboard Terra for evaluating the DARF over the Amazonia and cerrado regions. As CERES relies on angular distribution models (ADM) for estimating the upward flux at the TOA, it is very hard to validate those flux retrievals. Up to date, the validation of these TOA fluxes has only been made indirectly, by comparing TOA fluxes retrieved by broadband radiometers aboard different satellites (Loeb et al., 2007). As previously discussed, the use of different ADMs to convert broadband radiance measurements into flux may introduce large differences in the calculated DARF using satellite remote sensors (Patadia and Christopher, 2014). We have applied a correction to the DARF based on Patadia et al. (2011) empirical ADMs that accounts for the influence of aerosols in the anisotropy of scattered radiation. Nevertheless, those new angular distribution functions are also not validated and, since there are no instruments that directly measure the upward flux at the TOA, it is not possible to truly validate neither CERES ADMs nor Patadia's empirical ADMs.

As an attempt to indirectly validate the DARF results obtained here, we compared the DARF, calculated in this work, with both ground-based measurements and radiative transfer forcing estimates. In section 4.1 we analyzed the intercomparison between CERES-MODIS forcings, with those reported by AERONET's (AErosol RObotic NETwork) radiative forcing product. In section 4.2, CERES-MODIS forcings were compared with radiative forcing evaluations computed using SBDART (Santa Barbara DISORT Atmospheric Radiative Transfer model) radiative transfer code (Richiazzi et al., 1998).

4.1 Intercomparison between CERES-MODIS and AERONET 24-h DARF

AERONET is one of the most successful ground-based global networks of sun/sky radiometers for studying and monitoring aerosol physical properties around the world (Holben et al., 1998). Direct and almucantar measurements from AERONET radiometers are used to retrieve AOD and several column averaged aerosol optical and physical properties in different spectral bands. Extinction measurements on the spectral channel centered at 940 nm are used to assess column water vapour (Halthore et al., 1997). In its inversion product version 2.0, AERONET provides cloud-free sky DARF estimates evaluated using the radiative transfer code GAME (Global Atmospheric Model) (Dubuisson et al., 1996). The aerosol and surface models used in GAME are based on mean column averaged aerosol optical properties retrieved by AERONET's inversion algorithm (Dubovik and King, 2000) and surface properties retrieved by MODIS bidirectional reflectance product (Lucht et al., 2000, Schaaf et al., 2002), respectively.

The CERES-MODIS DARF, calculated according to the methodology described in section 2.1, was compared with the DARF reported by AERONET's inversion product. For this, we selected forcing results, located within ± 25 km of the AERONET sites that operated in the Amazonia during the study period (Abracos Hill, Alta Floresta, Balbina, Belterra, Cuiabá, Ji-Paraná and Rio Branco). AERONET's almucantar measurements, needed to calculate the radiative forcing, are made only when the solar zenith angle is larger than 50° . However, during the dry season, at the time Terra overpasses the study region (around 10:30 local time), the solar zenith angle is on average around 33° . For this reason, there were no coincident instantaneous DARF retrievals from CERES-MODIS radiometers and AERONET sunphotometers. To compare the results, the instantaneous DARF, obtained by both CERES-MODIS and AERONET, were expanded to 24-h average DARF using the methodology

described in Sena et al., 2013. A comparison between the 24h-DARF at the TOA obtained using AERONET and CERES-MODIS is shown in Figure 6.

By applying a linear fit to the data points of Figure 6, we see that the 24h-DARF derived from CERES-MODIS relates with the 24h-DARF reported by AERONET through the following equation:

$$DARF_{CERES-MODIS}^{24h} = (1.07 \pm 0.04)DARF_{AERONET}^{24h} - (0.0 \pm 0.6). \quad (5)$$

According to this equation, the agreement between CERES-MODIS and AERONET 24h-DARF is acceptable within the standard deviations of the fitted parameters. This is a remarkable result, since the 24h-DARF retrievals, showed in Figure 6, were obtained by applying completely different methodologies, and using different instruments. AERONET sunphotometers are at the surface and CERES-MODIS instruments are at 705 km aboard Terra satellite both looking at the atmospheric column. Besides that, as explained above, the instantaneous observations that were used to calculate the 24h-DARF, compared in our analysis, were performed at different hours of the day. All those differences contribute to the dispersion of about 5 W/m² around the adjusted line. The uncertainties involved in the surface and aerosol optical models used in GAME's radiative transfer code to calculate AERONET's DARF can also contribute to this dispersion. These results indicate a high agreement between the 24h-DARF obtained by these two independent procedures.

4.2 Intercomparison between CERES-MODIS and SBDART Instantaneous DARF

It is also important to intercompare satellite remote sensing retrievals with ground based measurements. In order to properly do that, we compare CERES-MODIS data at the TOA with SolRad-NET (Solar Radiation Network) pyranometers at the bottom of the atmosphere (BOA), using SBDART calculations to link BOA to TOA. To formulate the surface models used in SBDART, we selected 50 km x 50 km areas centred at the AERONET stations listed in Section 4.1. For each selected area, the spectral surface albedo was obtained from the linear interpolation of MODIS MCD43B1 surface albedo retrievals in 7 wavelengths (Lucht et al., 2000, Schaaf et al., 2002). The aerosol models used in these simulations were built using daily averages of intrinsic aerosol optical properties retrieved by AERONET. The aerosol optical depth and column water vapour measured by AERONET sunphotometers within $\pm 1/2$

hour of Terra's timepass over each site were also used as inputs in the radiative transfer code. The shortwave downward flux at the surface and the DARF at the TOA were computed by SBDART and compared with ground-based sensors solar flux measurements and with CERES-MODIS DARF, respectively.

Figure 7 shows the comparison between the downward flux at the surface ($F_{\downarrow BOA}$) calculated by SBDART between 0.3 and 2.8 μm and coincident solar flux measurements at the surface in the same spectral range from SolRad-NET pyranometers, that are collocated with AERONET sunphotometers. A linear fit of the downward flux measured by the pyranometer at the surface ($F_{BOA}^{PYRANOMETER}$) and calculated by SBDART (F_{BOA}^{SBDART}) indicate that these variables are related through the following equation:

$$F_{BOA}^{PYRANOMETER} = (1.00 \pm 0.04)F_{BOA}^{SBDART} - (20 \pm 27). \quad (6)$$

Equation 6 shows that the agreement between calculated and measured BOA fluxes is acceptable within the standard deviations. The apparent mismatch of about 20 W/m^2 between the calculated and measured values represents approximately 2.2% of the downward flux at the surface, and this is close to the instrumental uncertainty of the pyranometer, reported as 2%. These results show a good agreement between the downward irradiance at the surface, calculated using SBDART and SolRad-NET pyranometer measurements.

The intercomparison between the instantaneous TOA DARF obtained using CERES-MODIS and calculated using SBDART is shown in Figure 8. The data points in this graph have a dispersion of about 10 W/m^2 around the 1:1 line. A linear fit of the data plotted in Figure 8 shows that the instantaneous TOA DARF obtained from CERES-MODIS and from SBDART relate through the following equation:

$$DARF_{CERES-MODIS} = (0.86 \pm 0.06)DARF_{SBDART} - (6 \pm 2). \quad (7)$$

Several issues in this comparison must be taken into account. First the upward flux is strongly influenced by the surface reflection. MODIS sensor presents low spectral resolution in the shortwave spectrum and this limits the surface albedo model used as input in SBDART. Secondly, the atmosphere has to be taken into account twice: on the downward and upward path. This amplifies any inaccuracy in the optical properties assumed in the SBDART calculations.

Small deviations in the estimates of aerosol single scattering albedo can generate large differences in the forcing calculated by radiative transfer codes (Loeb and Su, 2010, Boucher et al., 2013). To assess the impact of the uncertainties associated with different single scattering albedo values, the 24h-DARF was computed in SBDART as a function of AOD at 550 nm for different values of single scattering albedo at 440 nm ($\omega_0=0.89, 0.92$ and 0.95) (Figure 9). The differences of ± 0.03 in ω_0 , used in these simulations, correspond to the uncertainty of the single scattering albedo inverted by AERONET.

According to Figure 9, a variability of 0.03 in the estimate of the single scattering albedo for the mean AOD observed over the Amazonia (0.2 to 0.4) would affect the 24h-DARF in about 1 to 2 W/m^2 . To evaluate if these values are consistent with the 24h-DARF variation observed by AERONET, the database was divided in AOD bins of 0.05 and the standard deviation of AERONET's 24h-DARF on each bin was analyzed. This analysis showed that for AOD varying from 0.2 to 0.4, the standard deviation of AERONET's 24h-DARF on each bin varied between 1.5 and 2.7 W/m^2 . This variation is higher than the one obtained using SBDART, because in those simulations, only single scattering albedo was varied and other aerosol and atmospheric properties were fixed. However, there are other variables that influence the 24h-DARF observed by AERONET besides single scattering albedo, such as scattering phase function, size distribution and atmospheric water vapor content. These values are very significant and they show that aerosol single scattering albedo is a critical parameter to accurately assess DARF.

Considering all potential sources of uncertainties on aerosol and surface albedo models used in SBDART to compute the DARF, it is possible to consider the comparison showed on Figure 8 as satisfactory. It is important to note that this validation consists of an indirect comparison, since, as previously discussed, it is not possible to obtain the flux at the TOA by direct methods.

5 Summary and conclusions

This work proposed a new methodology for assessing the direct radiative forcing of biomass burning aerosols over a large area of Amazonia using satellite remote sensing. Ten years of simultaneous CERES and MODIS retrievals, from 2000 to 2009, were used in this evaluation.

1 An important correction (Patadia and Christopher, 2014) was applied to the DARF, to account
2 for the anisotropic scattering of smoke aerosols.

3 The spatial and temporal distributions of the mean daily DARF were analysed. Those analysis
4 showed that due to the wind dynamics and fast transport of particles along the Amazon Basin,
5 the spatial distribution of the DARF may considerably change even during short periods of
6 time. The DARF varies strongly along the biomass burning season, showing up to 20 W/m²
7 daily variation. The intraseasonal behaviour of the DARF also varied significantly from year
8 to year due to different burning intensity associated with different climatic conditions and
9 other socioeconomical changes (Davidson et al., 2012).

10 The average of DARF during the biomass burning season were computed and compared with
11 DARF results obtained in a previous study (Sena et al., 2013). This comparison showed a
12 mean difference of about 3 W/m² on the DARF, depending on the methodology applied. This
13 difference was mainly caused by two factors: i) the difference in the reference used to
14 represent the clean scene in these two methodologies, and ii) the fact that, before 2005,
15 CERES-SSF product contains properties of aerosols from an older MODIS collection
16 (collection 4), which overestimates the forcing computed for those years when the previous
17 methodology is applied.

18 An important part of our efforts focused on linking satellite remote sensing with ground based
19 aerosol and radiation flux measurements. The DARF evaluated using the new methodology
20 proposed in this work was compared with AERONET and SBDART DARF assessments. The
21 results obtained from those intercomparisons were very satisfactory. This comparison also
22 indicates the importance of taking into account the angular distribution model corrections
23 proposed by Patadia and Christopher, 2014, and used in the present study. To our knowledge,
24 this was the first time satellite remote sensing assessments of the DARF were compared with
25 ground based DARF estimates.

26 The new methodology introduced in this work provided a large scale assessment of the direct
27 radiative forcing of biomass burning aerosols over the Amazonia at higher temporal
28 resolution than previous studies. It also showed an advantage over previous approaches for
29 evaluating the DARF using satellite remote sensing, because it considerably reduces the
30 statistical noise in the estimates of the DARF, resulting in a better correlation between DARF
31 and AOD, compared to previous assessments. This new methodology could also be applied to

1 assess the DARF in other places of the world under urban or biomass burning aerosol
2 influences, if suitable and robust aerosol optical parameters are available.

4 **Acknowledgements**

5 The authors would like to thank the Atmospheric Science Data Center at the NASA Langley
6 Research Center, for the processing and availability of CERES-SSF data. We thank Leandro
7 Mariano and Otaviano Helene for the helpful discussions on uncertainties. We also thank
8 FAPESP scholarships associated with the projects 2009/08442-7 and 2013/08582-9. This
9 research was funded by the FAPESP projects 2008/58100-2, 2013/05014-0 and CNPq project
10 457843/2013-6 and 475735-2012-9. We thank Alcides C. Ribeiro, Ana L. Loureiro, Fábio de
11 Oliveira Jorge and Simara Moraes for technical support. We thank Brent Holben, Joel Schafer
12 and Fernando Moraes for support on long term AERONET operations in Amazonia.

References

- Albrecht, B. A.: Aerosols, cloud microphysics, and fractional cloudiness. *Science*, 245(4923), 1227-1230, 1989.
- Andreae, M.O., Artaxo P., Fischer, H., Freitas, S.R., Grégoire, J. M., Hansel, A., Hoor, P., Kormann, R., Krejci, R., Lange, L., Lelieveld, J., Lindinger, W., Longo, K., Peters, W., de Reus, M., Scheeren, B., Dias, M., Strom, J., van Velthoven, P. F J., and Williams, J.: Transport of biomass burning smoke to the upper troposphere by deep convection in the equatorial region. *Geophysical Research Letters*, Vol. 28, 6, 951-954, doi: 10.1029/2000GL012391, 2001.
- Andreae, M O., Artaxo, P., Brandao, C., Carswell, F E., Ciccioli, P., da Costa, A L., Culf, A D., Esteves, J L., Gash, J. H C., Grace, J., Kabat, P., Lelieveld, J., Malhi, Y., Manzi, A O., Meixner, F X., Nobre, A D., Nobre, C., Ruivo, M., Silva-Dias, M A., Stefani, P., Valentini, R., von Jouanne, J., and Waterloo, M J.: Biogeochemical cycling of carbon, water, energy, trace gases, and aerosols in Amazonia: The LBA-EUSTACH experiments, *J. Geophys. Res.-Atmos.*, 107, 8066, doi:10.1029/2001JD000524, 2002.
- Andreae, M.O., D. Rosenfeld, P. Artaxo, A. A. Costa, G. P. Frank, K. M. Longo, and M. A. F. Silva-Dias, Smoking rain clouds over the Amazon. *Science*, Vol. 303, (5662) 1337-1342, 2004.
- Andreae, M. O.: Aerosols before pollution, *Science*, 315(5808), 50-51, 2007.
- Artaxo, P., Martins, J V., Yamasoe, M A., Procopio, A S., Pauliquevis, T M., Andreae, M O., Guyon, P., Gatti, L V., and Leal, A. M C.: Physical and chemical properties of aerosols in the wet and dry seasons in Rondonia, Amazonia, *J. Geophys. Res.-Atmos.*, 107, LBA 49-1–LBA 49-14, doi: 10.1029/2001JD000666, 2002.
- Artaxo, P., Rizzo, L. V., Paixao, M., de Lucca, S., Oliveira, P. H., Lara, L. L., Wiedemann, K. T., Andreae, M. O., Holben, B., Schafer, J., Correia, A. L., and Pauliquevis, T. M.: Aerosol particles in Amazonia: their composition, role in the radiation balance, cloud formation, and nutrient cycles, *Geophysical Monograph Series*, 186, 233–250, doi:10.1029/2008GM000778, 2009.

1 Artaxo, P., Rizzo, L. V., Brito, J. F., Barbosa, H. M. J., Arana, A., Sena, E. T., Cirino, G. G.,
2 Bastos, W., Martin, S. T., and Andreae, M. O.: Atmospheric aerosols in Amazonia and land
3 use change: from natural biogenic to biomass burning conditions, *Faraday Discuss.*, 165, 203–
4 235, doi:10.1039/C3FD00052D, 2013.

5 Betts, R. A., Malhi, Y. and Roberts, J. T.: The future of the Amazon: new perspectives from
6 climate, ecosystem and social sciences. *Philosophical Transactions of the Royal Society B:*
7 *Biological Sciences*, 363(1498), 1729-1735, 2008.

8 Boucher, O., D. Randall, P. Artaxo, C. Bretherton, G. Feingold, P. Forster, V.-M. Kerminen,
9 Y. Kondo, H. Liao, U. Lohmann, P. Rasch, S. K. Satheesh, S. Sherwood, B. Stevens and X.
10 Y. Zhang, 2013: Clouds and Aerosols. In: *Climate Change 2013: The Physical Science Basis.*
11 *Contribution of Working Group I to the Fifth Assessment Report of the Intergovernmental*
12 *Panel on Climate Change* [Stocker, T. F., D. Qin, G.-K. Plattner, M. Tignor, S. K. Allen, J.
13 Boschung, A. Nauels, Y. Xia, V. Bex and P. M. Midgley (eds.)], 571-657, Cambridge
14 University Press, Cambridge, United Kingdom and New York, NY, USA.

15 Bowman, D. M. J. S., Balch, J. K., Artaxo, P., Bond, W. J., Carlson, J. M., Cochrane, M. A.,
16 D’Antonio, C. M., Defries, R. S., Doyle, J. C., Harrison, S. P., Johnston, F. H., Keeley, J. E.,
17 Krawchuk, M. A., Kull, C. A., Marston, J. B., Moritz, M. A., Prentice, I. C., Roos, C. I.,
18 Scott, A. C., Swetnam, T. W., van der Werf, G. R. and Pyne, S. J.: Fire in the Earth system.,
19 *Science*, 324(5926), 481-4, doi:10.1126/science.1163886, 2009.

20 Charlson, R. J., Schwartz, S. E., Hales, J. M., Cess, R. D., Coakley, J. J., Hansen, J. E.,
21 Hofmann, D. J.: Climate forcing by anthropogenic aerosols. *Science*, 255(5043), 423-430,
22 1992.

23 Christopher, S. A.: Satellite remote sensing methods for estimating clear Sky shortwave Top
24 of atmosphere fluxes used for aerosol studies over the global oceans. *Remote Sensing of*
25 *Environment*, 115(12), 3002-3006, 2011.

26 Chylek, P. and Wong, J.: Effect of absorbing aerosols on global radiation budget. *Geophysical*
27 *research letters*, 22(8), 929-931, 1995.

1 Coakley, J. A., Bernstein, R. L. and Durkee, P. A.: Effect of ship-stack effluents on cloud
2 reflectivity. *Science*, 237(4818), 1020-1022, 1987.

3 Davidson, E. A. and Artaxo P.: Globally significant changes in biological processes of the
4 Amazon Basin: Results of the Large-scale Biosphere-Atmosphere Experiment. *Global*
5 *Change Biology*, 10(5), 1–11, doi: 10.1111/j.1529-8817.2003.00779.x, 2004.

6 Davidson, E. A., Araújo, A. C., Artaxo, P., Balch, J. K., Brown, I. F., Bustamante, M. M. C.,
7 Coe, M. T., DeFries, R. S., Keller, M., Longo, M., Munger, J. W., Schroeder, W., Soares-
8 Filho, B. S., Souza, C. M., and Wofsy, S. C.: The Amazon Basin in Transition. *Nature*, 481,
9 321-328, doi:10.1038/nature10717, 2012.

10 Dubovik, O. and King, M. D.: A flexible inversion algorithm for retrieval of aerosol optical
11 properties from Sun and sky radiance measurements, *Journal of Geophysical Research*,
12 105(D16), 20673-20696, doi:10.1029/2000JD900282, 2000.

13 Dubovik, O., Holben B., Eck T., Smirnov A., Kaufman Y., King M., Tanré D., and Slutsker
14 I.: Variability of absorption and optical properties of key aerosol types observed in worldwide
15 locations, *Journal of the Atmospheric Sciences*, 59 (3), 590-608, 2002.

16 Dubuisson, P., Buriez, J. C., and Fouquart, Y.: High spectral resolution solar radiative transfer
17 in absorbing and scattering media: Application to the satellite simulation, *J. Quant. Spectrosc.*
18 *Radiat. Transfer*. 55, 103–126, 1996.

19 Echalar, F., Artaxo, P., Martins, J. V., Yamasoe, M., Gerab, F., Maenhaut, W., and Holben,
20 B.: Long-term monitoring of atmospheric aerosols in the amazon basin: Source identification
21 and apportionment. *Journal of Geophysical Research*, 103(D24):31849-31864, 1998.

22 Eck, T. F., B. N. Holben, J. S. Reid, N. T. O'Neill, J. S. Schafer, O. Dubovik, A. Smirnov,
23 M.A. Yamasoe, and P. Artaxo, High aerosol optical depth biomass burning events: a
24 comparison of optical properties for different source regions. *Geophysical Research Letter*,
25 30, 20, 2035, doi: 10.1029/2003GL017861, 2003.

26 Edwards, D. P., Emmons, L. K., Gille, J. C., Chu, A., Attié, J. L., Giglio, L., Wood, S. W.,
27 Haywood, J., Deeter, M. N., Massie, S. T., Ziskin, D. C. and Drummond, J. R.: Satellite

1 observed pollution from Southern Hemisphere biomass burning. *Journal of Geophysical*
2 *Research: Atmospheres*, 111, D14312, doi:10.1029/2005JD006655, 2006.

3 Feng, N. and Christopher, S. A.: Clear sky direct radiative effects of aerosols over Southeast
4 Asia based on satellite observations and radiative transfer calculations. *Remote Sensing of*
5 *Environment*, 152, 333-344, 2014.

6 Freitas, S. R., K. M. Longo, M. A. F. Silva Dias, P. L. Silva Dias, R. Chatfield, E. Prins, P.
7 Artaxo and F. S. Recuero, Monitoring the Transport of Biomass Burning Emissions in South
8 America. *Environmental Fluid Mechanics*, Vol. 5, No. 1, pg. 135-167, doi: 10.1007/s10652-
9 005-0243-7, 2005.

10 Freitas, S. R., Longo, K. M., Silva Dias, M. A. F., Chatfield, R., Silva Dias, P., Artaxo, P., ...
11 & Panetta, J., The Coupled Aerosol and Tracer Transport model to the Brazilian
12 developments on the Regional Atmospheric Modeling System (CATT-BRAMS)–Part 1:
13 Model description and evaluation, *Atmospheric Chemistry and Physics*, 9(8), 2843-2861,
14 2009.

15 Halthore, R., Eck, T., Holben, B., and Markham, B.: Sun photometric measurements of
16 atmospheric water vapor column abundance in the 940-nm band, *Journal of Geophysical*
17 *Research*, 102, 4343-4352, 1997.

18 Haywood, J. and Boucher, O.: Estimates of the direct and indirect radiative forcing due to
19 tropospheric aerosols: A review, *Reviews of Geophysics*, 38, 513–543,
20 doi:10.1029/1999RG000078, 2000.

21 Holben, B. N., Setzer, A., Eck, T. F., Pereira, A., and Slutsker, I.: Effect of dry-season
22 biomass burning on Amazon basin aerosol concentrations and optical properties, 1992–1994,
23 *J. Geophys. Res.-Atmos.*, 101, 19465–19481, doi:10.1029/96jd01114, 1996.

24 Holben, B. N., Eck, T. F., Slutsker, I., Tanre, D., Buis, J. P., Setzer, A., Vermote, E., Reagan,
25 J. A., Kaufman, Y. J., Nakajima, T., Lavenu, F., Jankowiak, I. and Smirnov, A.: AERONET –
26 A Federated Instrument Network and Data Archive for Aerosol Characterization, *Remote*
27 *Sens. Environ.*, 66, 1–16, doi:10.1016/S0034-4257(98)00031-5, 1998.

1 King, M. D., Kaufman, Y. J., Menzel, W. and Tanre, D.: Remote sensing of cloud, aerosol,
2 and water vapor properties from the Moderate Resolution Imaging Spectrometer (MODIS).
3 Geoscience and Remote Sensing, IEEE Transactions on, 30(1), 2-27, 1992. Koren, I., Martins,
4 J. V., Remer, L. a and Afargan, H.: Smoke invigoration versus inhibition of clouds over the
5 Amazon., Science, 321(5891), 946-9, 2008.

6 Liou, K. N.: An introduction to atmospheric radiation (Vol. 84), Academic press, San Diego,
7 California, 2002.

8 Loeb, N. G., Kato, S., Loukachine, K. and Manalo-Smith, N.: Angular Distribution Models
9 for Top-of-Atmosphere Radiative Flux Estimation from the Clouds and the Earth's Radiant
10 Energy System Instrument on the Terra Satellite. Part I: Methodology, Journal of
11 Atmospheric and Oceanic Technology, 22(4), 338-351, doi:10.1175/JTECH1712.1, 2005.

12 Loeb, N. G., Kato, S., Loukachine, K., Manalo-Smith, N., and Doelling, D. R.: Angular
13 Distribution Models for Top-of-Atmosphere Radiative Flux Estimation from the Clouds and
14 the Earth's Radiant Energy System Instrument on the Terra Satellite. Part II: Validation, J.
15 Atmos. Ocean. Tech., 24, 564–584, doi:10.1175/JTECH1983.1, 2007.

16 Loeb, N. G. and Su, W.: Direct aerosol radiative forcing uncertainty based on a radiative
17 perturbation analysis. Journal of Climate, 23(19), 5288-5293, 2010.

18 Longo, K., S. R. de Freitas, M. O. Andreae, R. Yokelson, P. Artaxo. Biomass Burning in
19 Amazonia: Emissions, Long-Range Transport of Smoke and Its Regional and Remote
20 Impacts. In: Amazonia and Global Change, Ed. M. Keller, M. Bustamante, J. Gash, P. S.
21 Dias. American Geophysical Union, Geophysical Monograph 186, pg. 209-234, ISBN: 978-0-
22 87590-449-8, 2009, Washington, D. C., doi:10.1029/2008GM000778, 2009.

23 Lucht, W., Schaaf, C. B., and Strahler, A. H.: An algorithm for the retrieval of albedo from
24 space using semiempirical BRDF models, IEEE T. Geosci. Remote Sens., 38, 977–998,
25 doi:10.1109/36.841980, 2000.

26 Malhi, Y., Roberts, J. T., Betts, R. A., Killeen, T. J., Li, W., Nobre, C. A., Climate change,
27 deforestation, and the fate of the Amazon, Science, 319(5860), 169-172, 2008.

1 Marengo, J. A., Nobre, C. A., Tomasella, J., Oyama, M. D., Oliveira, G. S., Oliveira, R.,
2 Camargo, H., Alves, L. M., Brown, I.F., The drought of Amazonia in 2005, *J. Climate*, 21,
3 495-516, 2008.

4 Martin, S. T., Andreae M. O., Artaxo P., Baumgardner D., Chen Q., Goldstein A. H.,
5 Guenther A. B., Heald C. L., Mayol-Bracero O. L., McMurry P. H., Pauliquevis T., Pöschl
6 U., Prather K. A., Roberts G. C., Saleska S. R., Silva Dias M. A., Spracklen D. V., Swietlicki
7 E., and Trebs I.: Sources and Properties of Amazonian Aerosol Particles. *Review of*
8 *Geophysics*, Vol 48, Article number RG2002, DOI: 10.1029/2008RG000280, 2010.

9 Mishra, A. K., Lehahn, Y., Rudich and Y., Koren, I., Co-variability of smoke and fire in the
10 Amazon Basin. *Atmospheric Environment*, doi:10.1016/j.atmosenv.2015.03.007, 2015.

11 Morton, D. C., Defries, R. S., Randerson, J. T., Giglio, L., Schroeder, W. and Van Der Werf,
12 G. R.. Agricultural intensification increases deforestation fire activity in Amazonia. *Global*
13 *Change Biology*, 14(10), 2262-2275, <http://dx.doi.org/10.1111/j.1365-2486.2008.01652.x>,
14 2008.

15 Nobre, C. A., Mattos, L. F., Dereczynski, C. P., Tarasova, T. A., Trosnikov, I. V., Overview
16 of atmospheric conditions during the Smoke, Clouds, and Radiation-Brazil (SCAR-B) field
17 experiment, *Journal of Geophysical Research: Atmospheres* (1984–2012), 103(D24), 31809-
18 31820, 1998 Patadia, F., Gupta, P., Christopher, S. A., Reid, J. S.: A Multisensor satellite-
19 based assessment of biomass burning aerosol radiative impact over Amazonia. *J. Geophys.*
20 *Res*, 113, D12214, doi: 10.1029/2007JD009486, 2008.

21 Patadia, F., Christopher, S. A., and Zhang, J.: Development of empirical angular distribution
22 models for smoke aerosols: Methods. *Journal of Geophysical Research: Atmospheres*,
23 116(D14), 1984-2012, 2011.

24 Patadia, F. and Christopher, S. A.: Assessment of smoke shortwave radiative forcing using
25 empirical angular distribution models. *Remote Sensing of Environment*, 140, 233-240, 2014.

26 Prins, E. M., Feltz, J. M., Menzel, W. P., Ward, D. E.: An overview of goes-8 diurnal fire and
27 smoke results for scar-b and 1995 fire season in South America, *Journal of Geophysical*
28 *Research: Atmospheres*, 103(D24), 31821-31835, 1998.

1 Procopio, A., Artaxo, P., Kaufman, Y., Remer, L., Schafer, J. and Holben, B.: Multiyear
2 analysis of Amazonian biomass burning smoke radiative forcing of climate, *Geophys. Res.*
3 *Lett.*, 31(3), L03108–L03112, doi:10.1029/2003GL018646, 2004.

4 Remer, L. A., Kaufman, Y., Tanré, D., Mattoo, S., Chu, D. A., Martins, J. V., Li, R., Ichoku,
5 C., Levy, R., Kleidman, R., Eck, T. F., Vermote, E. and Holben, B. N.: The MODIS aerosol
6 algorithm, products and validation, *J. Atmos. Sci.*, 62(4), 947–973, 2005.

7 Ricchiazzi, P., Yang, S., Gautier, C., and Sowle, D.: SBDART: A Research and Teaching
8 Software Tool for Plane-Parallel Radiative Transfer in the Earth's Atmosphere, *B. Am.*
9 *Meteorol. Soc.*, 79, 2101–2114, 1998.

10 Ross, J., Hobbs P., and Holben B.: Radiative characteristics of regional hazes dominated by
11 smoke from biomass burning in Brazil: Closure tests and direct radiative forcing, *Journal of*
12 *geophysical research*, 103 (D24), 31,925-31, 1998.

13 Salomonson, V. V., Barnes, W., Maymon, P. W., Montgomery, H. E., Ostrow, H.: MODIS:
14 Advanced facility instrument for studies of the Earth as a system, *Geoscience and Remote*
15 *Sensing*, *IEEE Transactions on*, 27(2), 145-153, 1989.

16 Satyamurty, P., da Costa, C. P. W., Manzi, A. O., Moisture source for the Amazon Basin: a
17 study of contrasting years. *Theoretical and applied climatology*, 111(1-2), 195-209,
18 2013. Schaaf, C. B., Gao, F., Strahler, A. H., Lucht, W., Li, X., Tsang, T., Strugnell, N. C.,
19 Zhang, X., Jin, Y., Muller, J.-P., Lewis, P., Barnsley, M., Hobson, P., Disney, M.,
20 Dunderdale, M., Doll, C., d'Entremont, R. P., Hu, B., Liang, S., Privette, J. L., and Roy, D.:
21 First operational BRDF, albedo nadir reflectance products from MODIS, *Remote Sens.*
22 *Environ.*, 83, 135–148, doi:10.1016/S0034-4257(02)00091-3, 2002.

23 Schafer, J. S., Eck, T. F., Holben, B. N., Artaxo, P., and Duarte, A.: Characterization of the
24 optical properties of atmospheric aerosols in Amazonia from long term AERONET
25 monitoring (1993–1995; 1999–2006), *J. Geophys. Res.-Atmos.*, 113, D04204,
26 doi:10.1029/2007JD009319, 2008.

1 Sena, E. T., Artaxo, P., and Correia, A. L.: Spatial variability of the direct radiative forcing of
2 biomass burning aerosols and the effects of land use change in Amazonia, *Atmos. Chem.*
3 *Phys.*, 13, 1261-1275, doi:10.5194/acp-13-1261-2013, 2013.

4 Smith, G. L.: Effects of time response on the point spread function of a scanning radiometer.
5 *Applied Optics*, 33(30), 7031-7037, 1994.

6 Stamnes, K., Tsay, S., Wiscombe, W., and Jayaweera, K.: Numerically stable algorithm for
7 discrete-ordinate-method radiative transfer in multiple scattering and emitting layered media,
8 *Appl. Optics*, 27, 2502–2509, 1988.

9 Sundström, A.-M., Arola, A., Kolmonen, P., Xue, Y., de Leeuw, G., and Kulmala, M.: On the
10 use of satellite remote sensing based approach for determining aerosol direct radiative effect
11 over land: a case study over China, *Atmos. Chem. Phys. Discuss.*, 14, 15113-15147,
12 doi:10.5194/acpd-14-15113-2014, 2014.

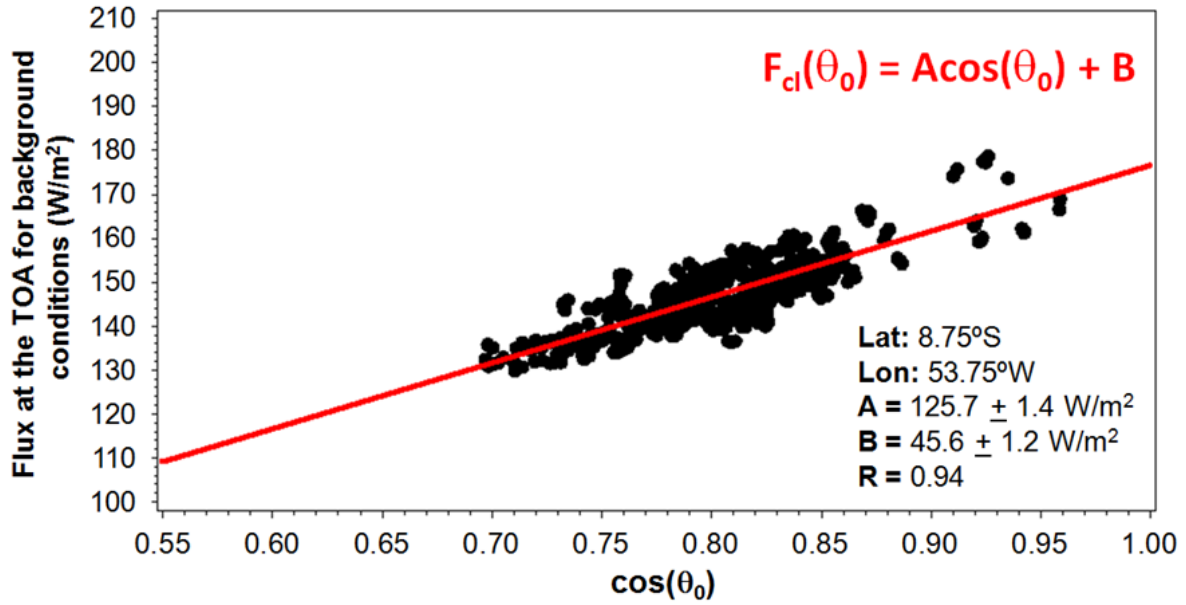
13 Ten Hoeve, J. E., Remer, L. A., Correia, A. L., and Jacobson, M. Z.: Recent shift from forest
14 to savanna burning in the Amazon Basin observed by satellite, *Environ. Res. Lett.*, 7, 024020,
15 doi:10.1088/1748-9326/7/2/024020, 2012.

16 Twomey, S.: The influence of pollution on the shortwave albedo of clouds, *J. Atmos. Sci.*, 34,
17 1149–1152, 1977.

18 Wielicki, B. A., Barkstrom B. R., Harrison E. F., Lee R. B., Smith G. L., and Cooper J. E.:
19 Clouds and the Earth's Radiant Energy System (CERES): An Earth observing system
20 experiment, *Bull. Am. Meteorol. Soc.*, 77, 853– 868, 1996.

21 Yu, H., Kaufman, Y. J., Chin, M., Feingold, G., Remer, L. A., Anderson, T. L., Balkanski, Y.,
22 Bellouin, N., Boucher, O., Christopher, S. A., DeCola, P., Kahn, R., Koch, D., Loeb, N.,
23 Reddy, M. S., Schulz, M., Takemura, T. and Zhou, M.: A review of measurement-based
24 assessments of the aerosol direct radiative effect and forcing. *Atmospheric Chemistry and*
25 *Physics*, 6(3), 613-666, 2006.

1 Zhang, J., Christopher, S. A., Remer, L. and Kaufman, Y. J.: Shortwave aerosol radiative
2 forcing over cloud-free oceans from Terra: 2. Seasonal and global distributions, J. Geophys.
3 Res, 110, D10S24, doi:10.1029/2004JD005009, 2005.
4



1
2 Figure 1: Example of the procedure used to obtain the flux at the top of the atmosphere
3 (TOA) for background conditions (F_{cl}) as a function of the solar zenith angle (θ_0) for a $0.5^\circ \times$
4 0.5° cell located in the Amazon Basin. In this example, four months worth of data over the
5 grid cell were used, from July to October, 2005.

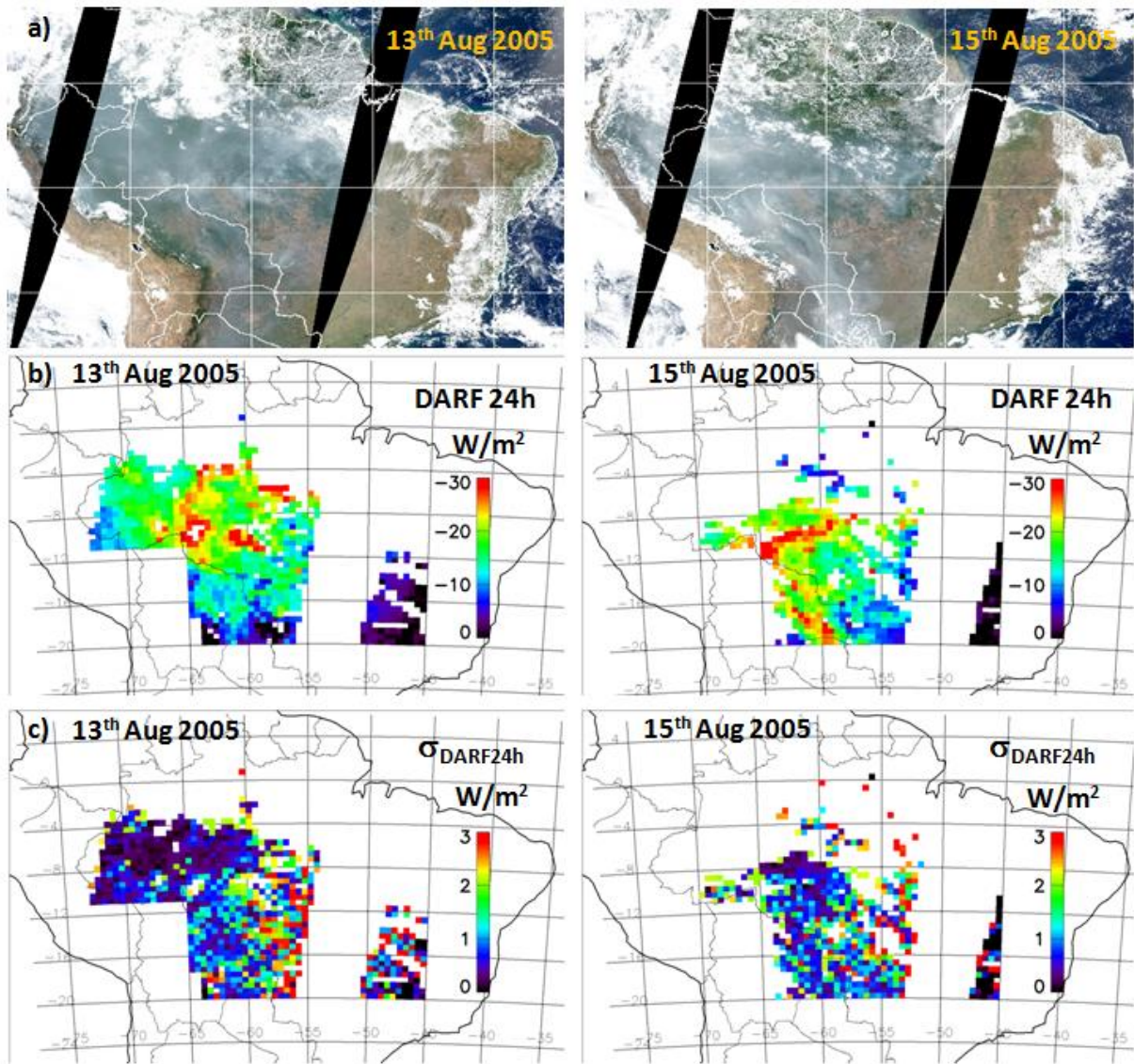


Figure 2: (a) Examples of composite MODIS RGB (red, green, blue) images over the Amazonia, (b) mean daily spatial distributions of the direct aerosol radiative forcing of aerosols (DARF24h), (c) and their uncertainties for 13th August 2005 (left) and 15th August 2005 (right).

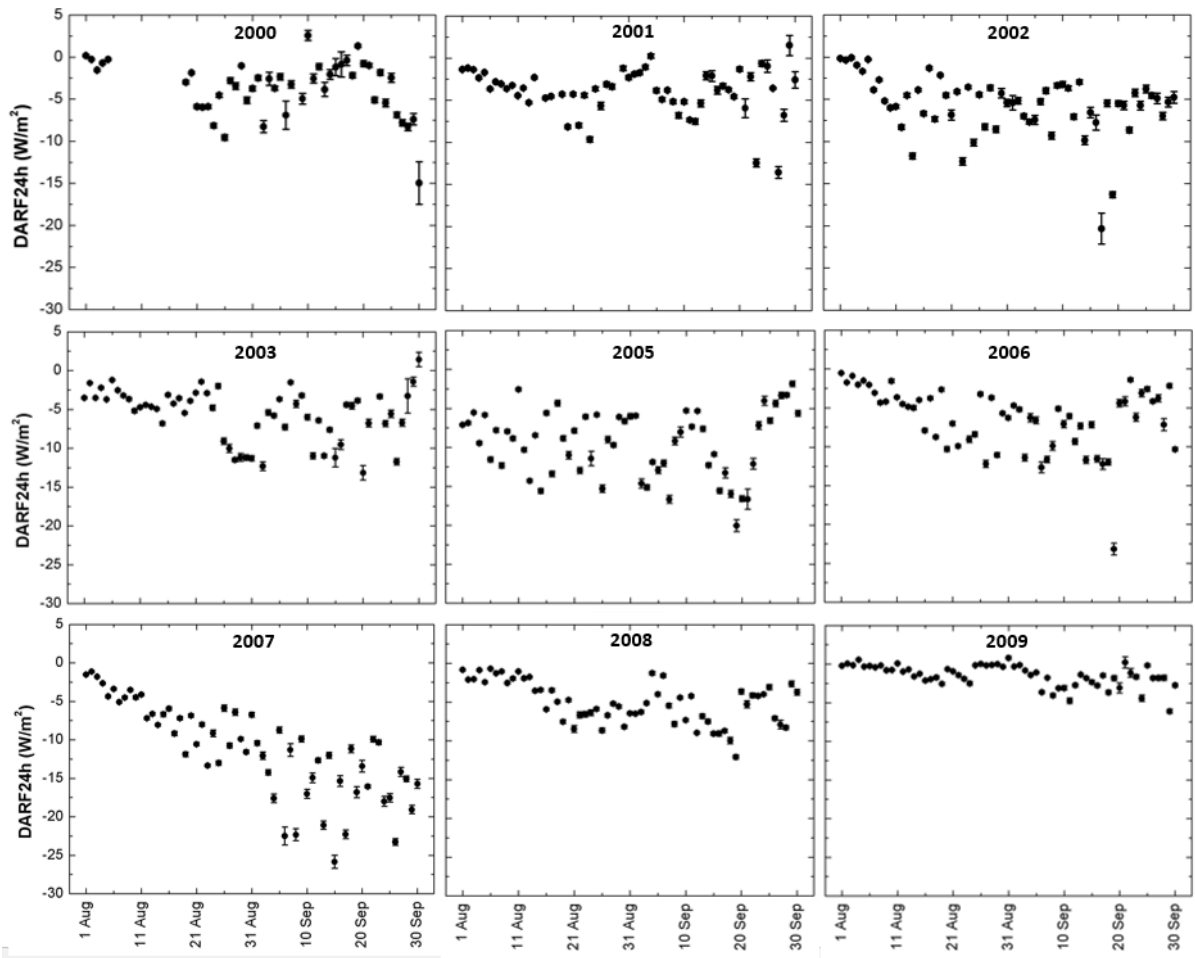


Figure 3: Temporal variability of the direct radiative forcing of aerosols (DARF24h) along the biomass burning season for: (a) 2005, (b) 2006 and (c) 2007.

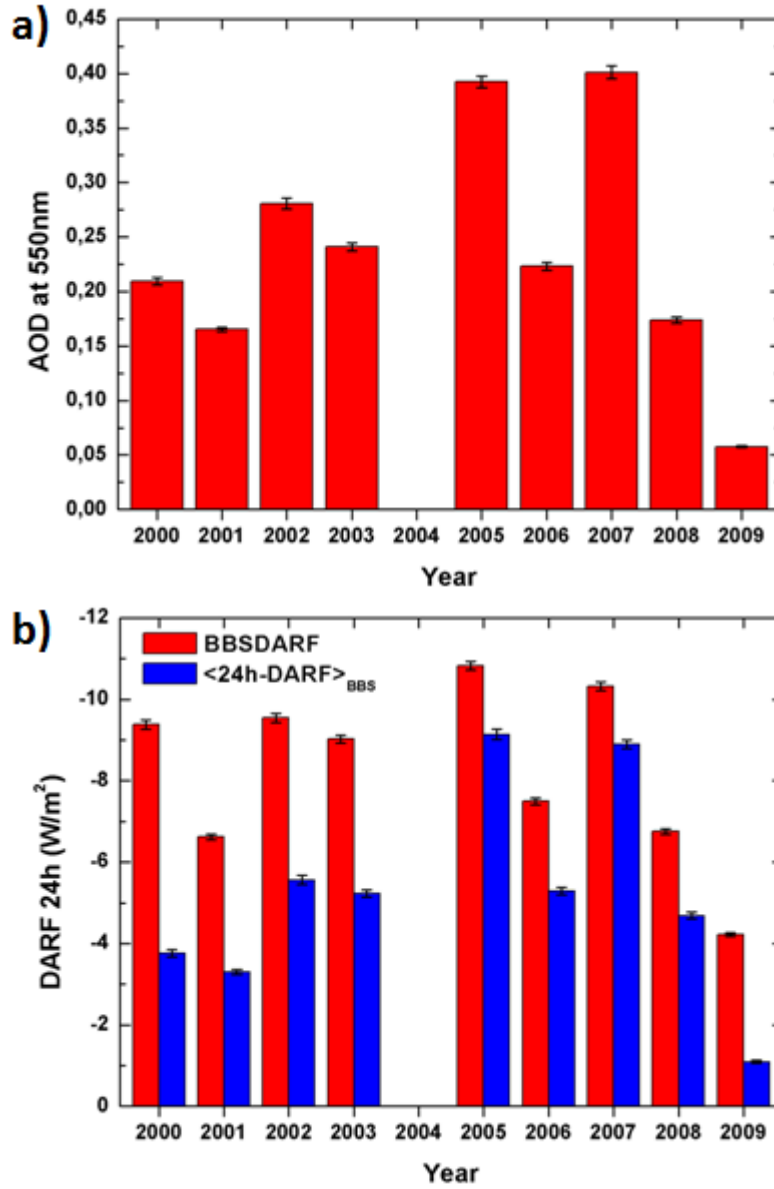
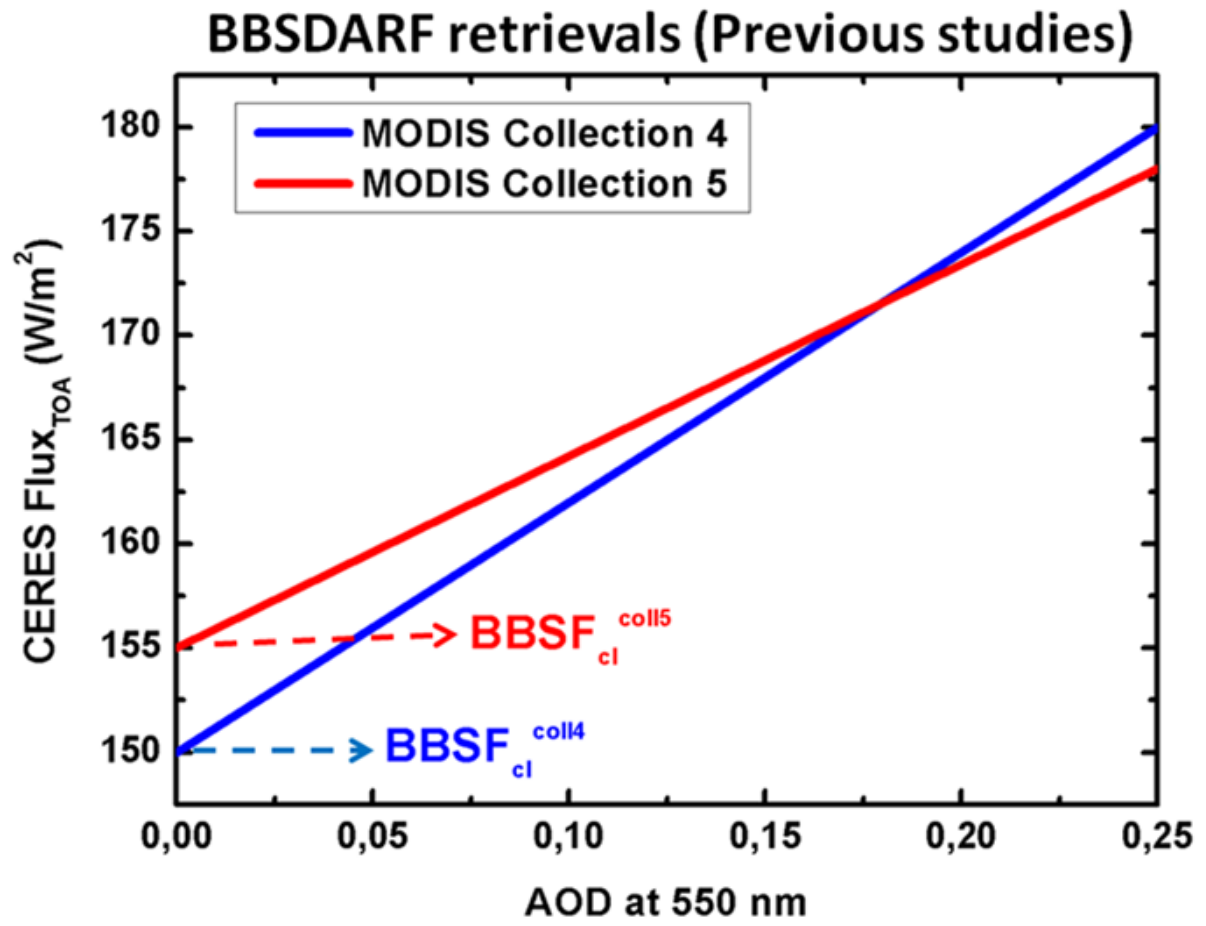


Figure 4: (a) MODIS

mean aerosol optical depth at 550 nm over Amazonia during the dry season (b) and mean direct aerosol radiative forcing of aerosols (DARF24h) during the peak of the biomass burning season (August to September) from 2000 to 2009 obtained by the methodology applied by Sena et al., 2013 (BBSDARF) and by the methodology proposed in this work ($\langle 24hDARF \rangle_{BBS}$).



1
 2 Figure 5: Schematic illustration of the differences in the linear fits of CERES flux at the top
 3 of the atmosphere (TOA) and MODIS collection 4 and collection 5 aerosol optical depth
 4 (AOD) at 550 nm. No real data was used in this figure.

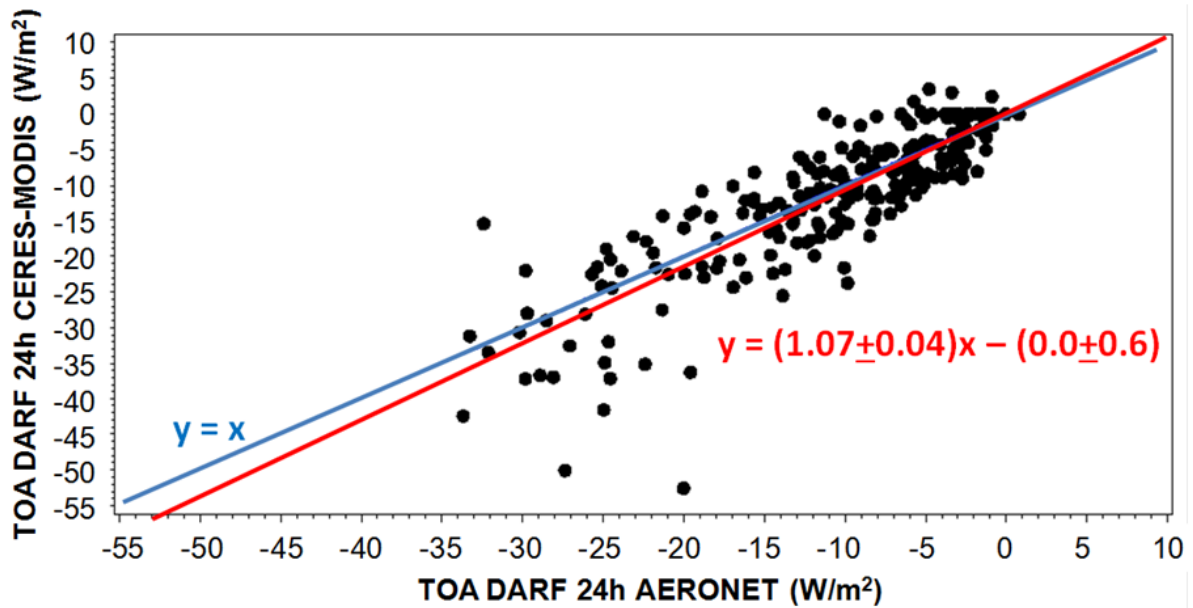


Figure 6: Intercomparison between the mean daily direct radiative forcing (DARF24h) at the top of the atmosphere (TOA) evaluated using CERES-MODIS and by AERONET inversion product.

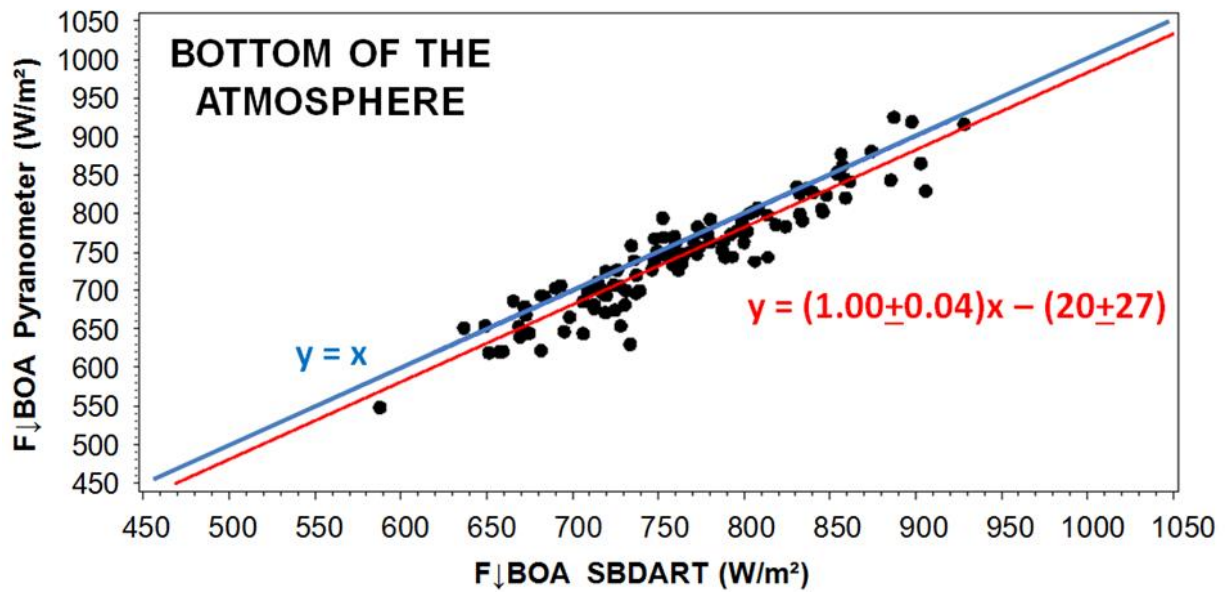
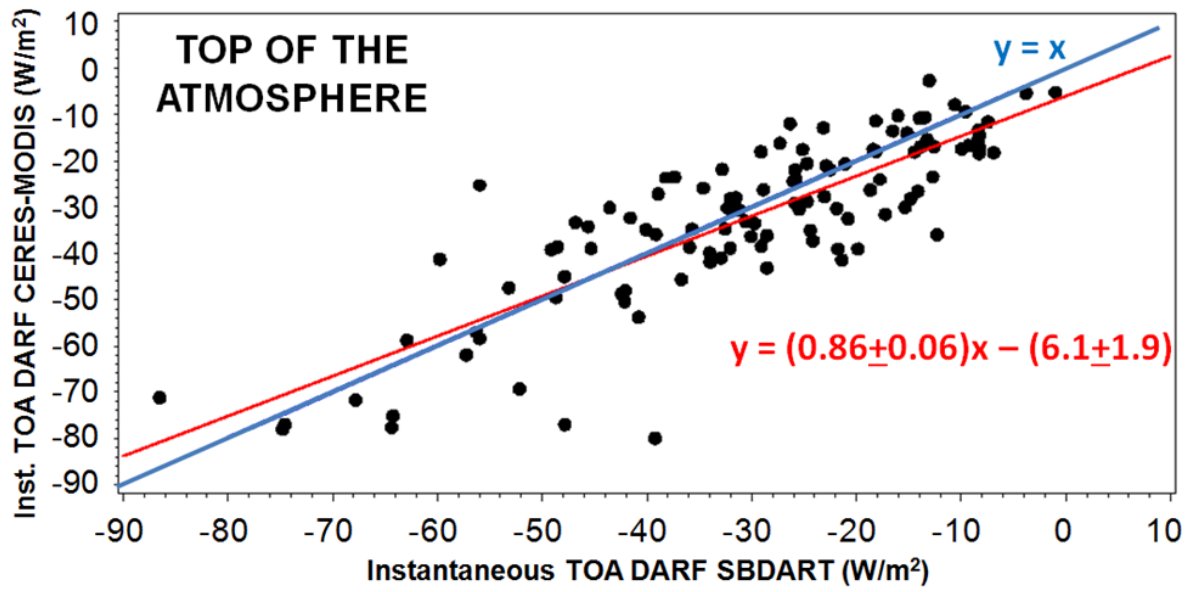
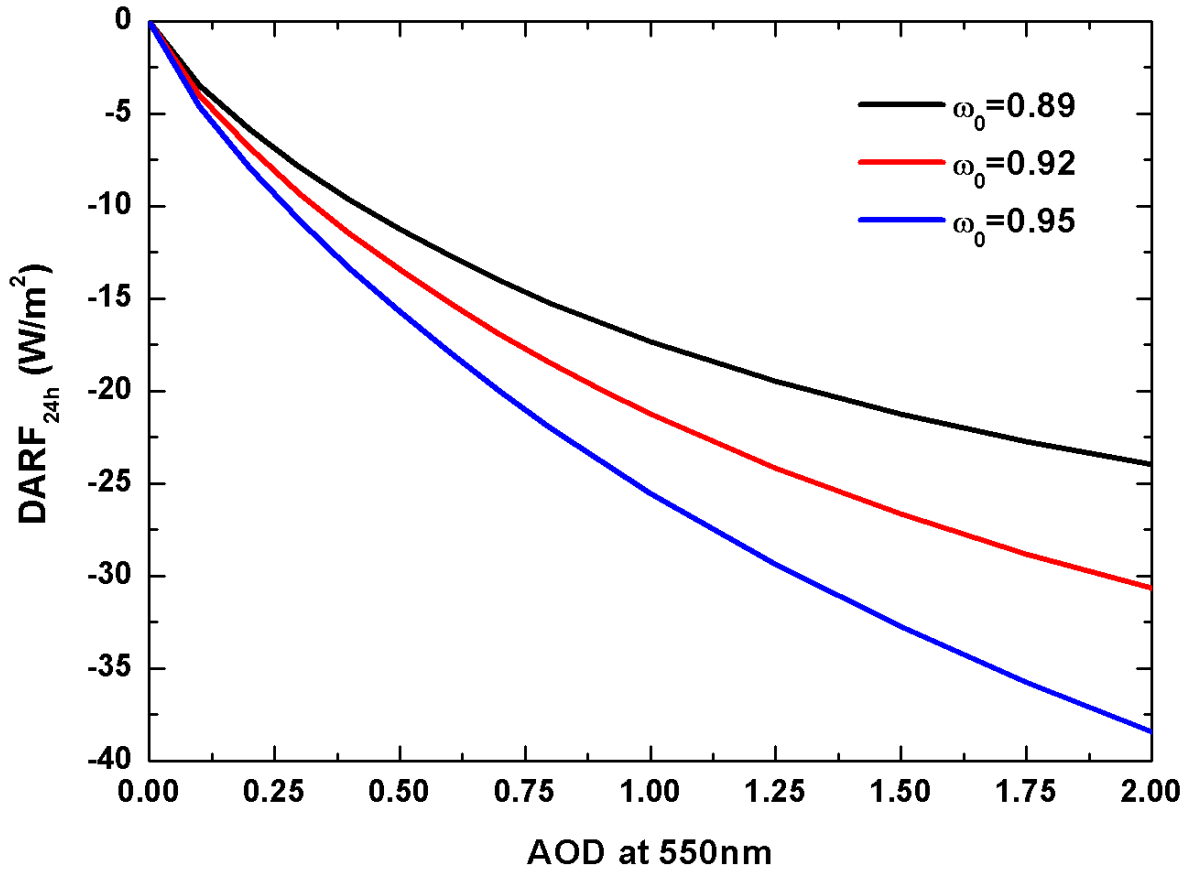


Figure 7: Intercomparison between the incoming flux in W/m² at the bottom of the atmosphere (BOA) measured by SolRad-NET pyranometers and modelled using AERONET and MODIS BRDF retrieved optical properties as inputs in SBDART.



1
2
3
4
5

Figure 8: Intercomparison between the instantaneous direct aerosol radiative forcing (DARF) at the top of the atmosphere (TOA) evaluated using CERES-MODIS and modelled using AERONET and MODIS BRDF retrieved optical properties as inputs in SBDART.



1
2 Figure 9: Direct radiative forcing of biomass burning aerosols (DARF_{24h}) over the forest as a
3 function of aerosol optical depth (AOD) at 550 nm and single scattering albedo (ω_0) at 440
4 nm according to radiative transfer calculations.